

Image Denoising Based on Adaptive Quincunx Wavelets

Miroslav Vrankić

Dept. of Electrical Engineering
Faculty of Engineering
University of Rijeka, Croatia
Miroslav.Vrankic@RITEH.hr

Damir Seršić

Dept. of Electronic Systems and Information Processing
Faculty of Electrical Engineering and Computing
University of Zagreb, Croatia
Damir.Sersic@FER.hr

Abstract—In this paper, we explore the use of nonseparable and adaptive wavelet decompositions for the purpose of image denoising. We apply the classical wavelet shrinkage methods on the wavelet coefficients obtained by using the adaptive wavelet transform defined on the quincunx grid. The wavelet transform is pixel-wise adaptive in all decomposition levels. While providing more compact representation of the analyzed image, the adaptive transform retains some useful properties of fixed transforms, such as numbers of vanishing moments of primal and dual wavelets. The adaptive wavelet decomposition is realized using the lifting scheme. For comparison purposes, the image denoising results are presented for both fixed and adaptive wavelet transforms.

Keywords—adaptive wavelets, image denoising, lifting scheme, quincunx, interpolating filters

I. INTRODUCTION

Wavelet shrinkage [1], [2] is a very simple, but efficient technique for image denoising. It relies on good localization and approximation properties of the wavelet transform. Image denoising via wavelet shrinkage is performed as follows: wavelet coefficients of the noisy image smaller than a given threshold are set to zero and the coefficients above the threshold are either left unchanged (hard thresholding) or reduced by the value of the threshold (soft thresholding). Afterwards, the noise-free image estimate is obtained through an inverse wavelet transform. The reason for effectiveness of such a procedure lies in the fact that in wavelet domain, a small number of high-valued detail coefficients represent areas around sharp transitions (edges) while the bulk of small and close to zero detail coefficients represents the smooth image regions.

In this paper, we employ a locally adaptive wavelet transform prior to denoising via wavelet shrinkage. The transform adapts itself to the local properties of the image, minimizing the energy of the wavelet detail coefficients for every pixel of the analyzed image. If the adaptation algorithm is robust enough regarding the noise, the adaptive wavelet shrinkage preserves better the original features of the image.

As a starting point, we have used quincunx interpolating filter banks designed by Kovacevic and Sweldens [4], based on the lifting scheme [5]. The usage of the lifting scheme enabled to transform the fixed wavelet filter bank into an adaptive wavelet filter bank structure. We have used quincunx

filter banks in order to have truly nonseparable wavelet decomposition that is, contrary to the wavelets defined on the separable grid, less biased in horizontal and vertical directions. Also, since the filter bank based on quincunx sampling consists of only two channels (compared to the four channels of the separable filter bank), it is much simpler and straightforward to introduce the adaptation.

II. ADAPTIVE QUINCUNX INTERPOLATING FILTER BANKS

Properties of a given wavelet decomposition are highly affected with the underlying sampling scheme, i.e. with the way the image samples are divided into a number of cosets (phases). The separable sampling scheme (Fig. 1 left) leads to dividing an image into four phases. In a similar manner the critically sampled filter bank used to realize the corresponding FWT will have four channels leading to one set of approximation coefficients and three sets (subimages, subbands) of detail coefficients for each decomposition level. The three detail subbands correspond to horizontal, vertical and diagonal details in the original image.

In the quincunx sampling scheme (Fig. 1 right) an image is being divided in only two distinct cosets. In the Fig. 1, the first coset is represented by gray circles and the second coset is represented by white circles. Such a sampling scheme is a basis for a two-channel critically sampled wavelet filter bank which results in one image of approximation coefficients and one image of detail coefficients for each decomposition level.

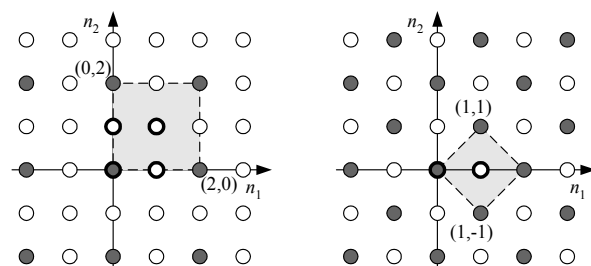


Fig. 1. Separable (left) and quincunx (right) sampling lattices. The unit cell for each lattice is outlined with a dashed line and the corresponding samples are bolded. Samples belonging to the first coset for the given sampling scheme are marked with gray circles. The number of cosets equals the number of samples belonging to the unit cell.

The lifting scheme typically consists of three stages (see Fig. 2): split, predict and update.

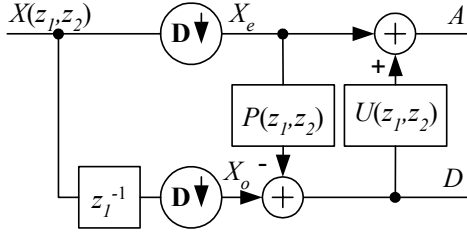


Fig. 2. Analysis filter bank based on the lifting scheme. The operator $D\downarrow$ represents two-dimensional downsampling.

In the split stage, an image is being split into a number of cosets (phases), depending on the sampling scheme used. For the case of quincunx sampling, the split stage divides an image into two cosets (phases) as shown in Fig. 1. Then, for each pixel in the second phase, the predict stage predicts its value based on a number of pixels from the first phase (Fig. 3). The resulting detail coefficients are calculated as a difference of a second image phase and the output of the prediction filter. In this way, wavelet detail coefficients are obtained as an error of predicting samples from the second image phase based on a number of their surrounding samples from the first image phase.

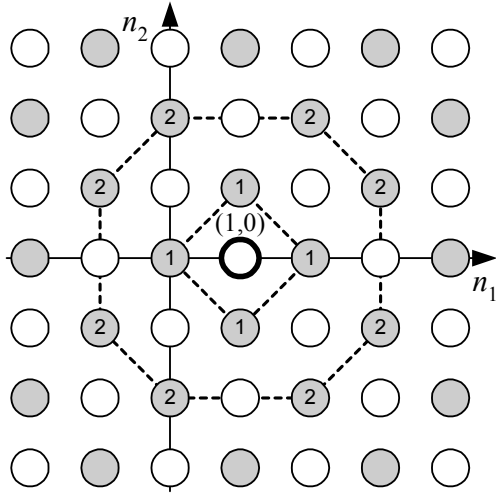


Fig. 3. A sample from the second quincunx phase (white circle marked bold) is being predicted based on a number of neighboring samples from the first phase (enumerated gray circles). Support of the prediction filter P_2 covers only four samples marked with 1. Prediction filter P_4 (fourth order prediction) uses samples marked with 1 together with samples marked with 2.

Finally, in the update stage, the U filter is used to update the value of the average wavelet coefficients by using the already calculated detail coefficients.

On the synthesis side, the reconstruction is easily performed by just inverting the order and signs of the predict and update steps. The first image phase is reconstructed by

subtracting the output of the update filter from the average wavelet coefficients. Then, the reconstructed first image phase is filtered with the prediction filter whose output is added to the wavelet detail coefficients resulting in the second image phase. The reconstructed image is obtained by simply joining together the two phases.

In our adaptive modification of the lifting scheme structure, the basic idea is to split the predict step into two parts [6]: the fixed prediction part and the adaptive prediction part as shown in Fig. 4, where P_2 and P_4 are the so-called Neville interpolating filters [4] of order 2 and 4 respectively:

$$\begin{aligned} P_2(z_1, z_2) &= (1 + z_1^{-1} + z_2^{-1} + z_1^{-1}z_2^{-1})/4, \\ U_2(z_1, z_2) &= P_2^*(z_1, z_2)/2 = (1 + z_1 + z_2 + z_1z_2)/8, \\ P_4(z_1, z_2) &= (10 + 10z_1^{-1} + 10z_2^{-1} + 10z_1^{-1}z_2^{-1} - \\ &\quad - z_1^{-2} - z_2^{-2} - z_1^{-2}z_2^{-1} - z_1^{-1}z_2^{-2} - z_1 - z_2 - z_1z_2^{-1} - z_1^{-1}z_2)/32. \end{aligned} \quad (1)$$

The adaptation in the second branch is introduced through the multiplier p whose value is being changed throughout the image in order to locally adapt the properties of the filter bank. The fixed prediction branch ensures the polynomial reconstruction property of the wavelet transform (number of vanishing moments), while the adaptive branch enables the wavelet decomposition to be tuned to the properties of the analyzed image without affecting the number of vanishing moments of the synthesis wavelet functions. This important property comes from the fact that the adaptive prediction branch $p(P_4 - P_2)$ always has the zero output for the inputs that are polynomials of order lower than 2, no matter what values the adaptive parameter p may take. As shown in [6], the adaptive prediction part can be composed of more than one adaptive prediction branch and also a similar structure can be employed to obtain an adaptive update step. For the sake of simplicity, in this paper we only use the simplest adaptive filter bank structure shown in Fig. 4.

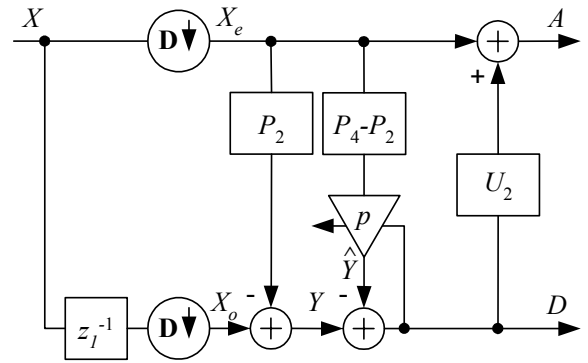


Fig. 4. Adaptive analysis quincunx filter bank. The predict step consists of two parts: fixed prediction branch and the adaptive prediction branch

Since the decimated wavelet transform is not shift invariant, the denoising result will depend on the positions of the discontinuities in the image. Improved results can be obtained using the undecimated version of the given wavelet transform [3]. In this paper, we use the undecimated wavelet transforms only. In that case, the decimation operators are removed from the lifting scheme and the N -times quincunx-

upsampled versions of P and U filters are used, where N represents the decomposition level. This way, for higher (i.e. coarser) decomposition levels the corresponding filters' support widens.

In the adaptive prediction branch, we have used generalized 2D windowed least squares (LS) adaptation algorithm. It is used to improve the performance of the prediction step by minimizing the squared prediction error. Since the wavelet detail coefficients are treated as an error of predicting samples from the second image phase based on a number of samples from the first phase, the minimization of the squared prediction error leads to minimizing the energy of the detail coefficients. The least squares solution for the p parameter has been calculated for every pixel of the analyzed image based on a window 5×5 pixels big that symmetrically surrounds the adaptation point.

Given the equation,

$$\mathbf{y} = \mathbf{A}p + \mathbf{e} = \hat{\mathbf{y}} + \mathbf{e}, \quad (2)$$

the LS solution for p is the one that minimizes $\|\mathbf{e}\|_2^2 = \|\mathbf{y} - \hat{\mathbf{y}}\|_2^2$, where \mathbf{y} is a vector that contains values of the signal in the lower branch after the subtraction of the P_2 filter output (see Fig. 4). Since the adaptation is based on a moving window that is 5×5 pixels large, the vector \mathbf{y} contains 25 entries. The \mathbf{A} matrix has 25 rows and 1 column (since the unknown p is just a scalar) and contains the values of the output of the P_4 - P_2 block.

It is well known that the solution to this problem is

$$p = (\mathbf{A}^T \mathbf{A})^{-1} \mathbf{A}^T \mathbf{y} \quad (3)$$

If each component of \mathbf{e} is a zero-mean, i.i.d. random variable with variance σ^2 , the estimator p is said to be a best linear unbiased estimator (BLUE) [7]. In the case that \mathbf{e} represents the colored noise with the covariance matrix $\mathbf{R} = E[\mathbf{e}\mathbf{e}^T]$ that is not diagonal, the BLUE solution is obtained as

$$p = (\mathbf{A}^T \mathbf{R}^{-1} \mathbf{A})^{-1} \mathbf{A}^T \mathbf{R}^{-1} \mathbf{y} \quad (4)$$

In the case of image denoising, the input image is obtained by adding the zero-mean Gaussian white noise to the original image. Since the noise in the signal \mathbf{y} has been colored after passing through the high-pass filter $1-P_2$, the appropriate covariance matrix \mathbf{R} has been constructed in order to obtain the estimate p whose value is least affected by the noise in the input image.

By moving the adaptation window, for each pixel of the analyzed image, one value of the p parameter has been calculated. Using the equation (4), the p parameters follow the features of the analyzed image and the remaining detail coefficients mostly correspond to the noise present in the image. By this approach, the important features of the image are expected to be mostly stored in the locally adapted wavelet functions, defined by the values of p parameters, while noise dominates in the detail coefficients. This way, in order to obtain the denoised image, much higher threshold can be used than in the case of using fixed filter banks.

III. EXPERIMENTAL SETUP

In the experiments, we have used eight-level adaptive undecimated wavelet decomposition. Detail wavelet coefficients from all decomposition levels have been either soft or hard thresholded. Since the employed filter bank is biorthogonal, different threshold weights have been applied for each decomposition level. For an analyzed image with additive Gaussian noise with standard deviation σ , the final threshold value is obtained as a weighted multiple of the noise deviation: $T_Q = N\sigma W$. The weights have been obtained empirically and for levels from 1 to 8 (finest to coarsest) they are: $W = \{2.5 \ 1.5 \ 0.9 \ 0.8 \ 0.7 \ 0.6 \ 0.5 \ 0.4\}$.

After thresholding of wavelet detail coefficients, the reconstructed image has been compared to the original (non-noisy) image. The peak signal to noise ratio (PSNR) has been used as a measure of denoising effectiveness.

For comparison purposes, the denoising results based on the fixed wavelets defined on the quincunx grid and fixed separable wavelets have been shown.

In the case of fixed quincunx wavelets, we have used second order prediction filter P_2 . Combined with the update filter U_2 , we have got a biorthogonal wavelet filter bank with 2 dual and 2 primal vanishing moments. For denoising, the eight-level wavelet decomposition has been performed together with the same thresholding as in the case of adaptive quincunx wavelets.

In the separable case, Daubechies wavelets of order two (*db2*) have been used to decompose an image into four decomposition levels. The threshold is obtained as a multiple of the noise deviation: $T_S = N\sigma$ and it is the same for all decomposition levels.

IV. RESULTS AND CONCLUSION

Fig. 5 shows the denoising results in terms of PSNR for various threshold levels. It shows that denoising performance improvement when using adaptive quincunx wavelets is relatively small (1dB at most) compared to fixed quincunx and separable wavelets. For the case of hard thresholding this improvement gets smaller as noise variance increases. The reason that the improvement is not greater lies in the fact that the (colored) noise is also present in the matrix \mathbf{A} of equation (4), which is supposed to be noiseless.

Still, in the right column of Fig. 5 ($\sigma = 20$), it can be seen that when the threshold value increases (more wavelet coefficients are being set to zero), the PSNR decreases faster for nonadaptive wavelet decompositions than for the case of adaptive wavelets. It means that in the adaptive wavelet case, the information on some features of the original image has been transferred to the p parameters and cannot be lost by thresholding the wavelet detail coefficients.

It is obvious that the generalized least squares approach represented by equation (4) cannot give the optimal results since it does not take into account that the colored noise is present in both channels of the filter bank. The solution to this problem might lie in the so-called errors-in-variable modeling and it is the topic of an ongoing research.

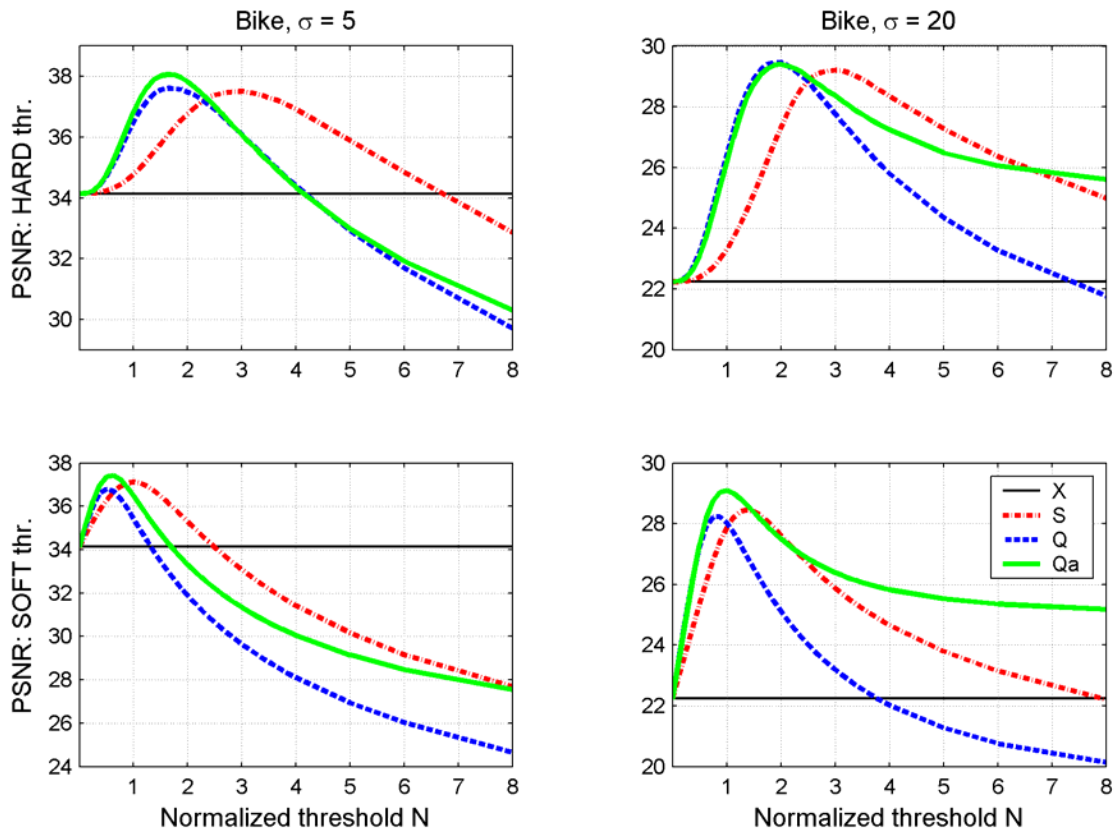


Fig. 5. Wavelet shrinkage results when denoising the Bike image with additive Gaussian noise with $\sigma = 5$ (first column) and $\sigma = 20$ (second column) obtained with separable wavelets (S), quincunx wavelets (Q) and adaptive quincunx wavelets (Qa). For Q and Qs, the threshold is $T_Q = N\sigma W$. For the separable case (S), $T_S = N\sigma$. First row: hard thresholding. Second row: soft thresholding.



Fig. 6. Part of the original Bike image 200x200 pixels big that has been used to test the denoising algorithms.

REFERENCES

- [1] D. Donoho and I. Johnstone, "Ideal Spatial Adaptation via Wavelet Shrinkage", *Biometrika*, vol. 81, pp. 425-455, 1994.
- [2] D. Donoho and I. Johnstone, "Adapting to Unknown Smoothness via Wavelet Shrinkage", *J. Amer. Stat. Assoc.*, vol. 90, pp. 1200-1224, 1995.
- [3] R. Coifman and D. Donoho, "Translation-invariant Denoising", in *Wavelets and Statistics*, A. Antoniadis and G. Oppenheim (eds.), Springer-Verlag, pp. 125-150, 1995.
- [4] J. Kovačević and W. Sweldens, "Wavelet Families of Increasing Order in Arbitrary Dimensions", *IEEE Trans. on Image Proc.*, vol. 9, no. 3, pp. 480-496, 2000.
- [5] W. Sweldens, "The lifting scheme: A custom-design construction of biorthogonal wavelets", *Appl. Comput. Harmon. Anal.*, 3(2):186-200, 1996
- [6] D. Sersic and M. Vrankic, "2-D Nonseparable Wavelet Filter Bank With Adaptive Filter Parameters", in *Proc. of EUSIPCO 2002*, vol I, pp. 137-140, 2002.
- [7] Simon Haykin, "Adaptive filter theory". Prentice-Hall Information and System Science Series. Prentice-Hall, Englewood Cliffs, New Jersey, 1986.